PHYSICAL REVIEW D **90,** 035019 (2014)

Radiative generation of lepton masses with the $U(1)'$ gauge symmetry

Hiroshi Okada[1,*] and Kei Yagyu[2,†]

[1]*School of Physics, KIAS, Seoul 130-722, Korea*

[2]*Department of Physics and Center for Mathematics and Theoretical Physics, National Central University, Chungli 32001, Taiwan, Republic of China*

(Received 17 May 2014; published 18 August 2014)

We revisit our previous model proposed by Okada and Yagyu [Phys. Rev. D 89, 053008 (2014)], in which lepton masses, except the tauon mass, are generated at the one-loop level in TeV-scale physics. Although in the previous work, rather large Yukawa coupling constants, i.e., greater than about 3, are required to reproduce the muon mass, we do not need to introduce such large $\mathcal{O}(1)$ couplings. In our model, masses for neutrinos (charged leptons) are generated by higher-dimensional operators with two isospin triplet (singlet and doublet) scalar fields, which are introduced at the one-loop level. Thus, the mass hierarchy between neutrinos and charged leptons can be naturally described by the difference in the number of vacuum expectation values of the triplet fields which must be much smaller than the vacuum expectation values of the doublet field due to the constraint from the electroweak rho parameter. Furthermore, the discrepancy in the measured muon anomalous magnetic moment $(g-2)$ from the prediction in the standard model is explained by new particle contributions at the one-loop level. The collider phenomenology is discussed, especially focusing on a signature from doubly charged scalar bosons at the LHC.

DOI: 10.1103/PhysRevD.90.035019 PACS numbers: 12.60.-i, 12.60.Fr, 95.35.+d

I. INTRODUCTION

The standard model (SM) can successfully describe almost all the phenomena at collider experiments even after the discovery of the Higgs boson at the LHC [1]. However, it is well known that there are phenomena which cannot be explained in the SM, such as the neutrino oscillations, the existence of dark matter (DM), and baryon asymmetry of the Universe. This strongly suggests that the SM should be replaced by a new physics model giving an explanation of these phenomena.

One of the attractive scenarios to explain tiny neutrino masses is obtained in radiative seesaw models, in which the dimension-five operator $\overline{L_L^c} L_L \Phi\Phi$, where L_L and Φ are, respectively, the left-handed lepton doublet and the Higgs doublet fields supplying Majorana-type neutrino masses, is generated through quantum levels. Thanks to a loop suppression factor, a new physics scale can be of order 1 TeV. Therefore, this class of models can be directly tested at collider experiments. Furthermore, a DM candidate can be naturally obtained[1] due to an unbroken discrete symmetry, which is necessary to enclose a loop diagram generating neutrino masses and to forbid lower order masses such as a tree-level Dirac neutrino mass.

So far, various models have been constructed in this line. The model by Krauss *et al.* has been proposed in the very early stage [4,5], in which neutrino masses are generated at the three-loop level, and its phenomenology at e^+e^- colliders has been discussed in Ref. [6]. Another simple model with one-loop induced neutrino masses has been constructed by Ma [7–9], and its extensions have also been discussed in Ref. [10]. The model by Aoki *et al.* [11–13] is the three-loop radiative seesaw model, where the successful scenario based on the electroweak baryogenesis [14] can be realized. Models with radiative generations for Dirac-type masses for neutrinos have been proposed in Ref. [15]. In addition to the above modes, there are a lot of papers proposing various types of radiative seesaw models [16,17].

Apart from neutrino masses, the masses of charged leptons are also so small compared to the electroweak scale, i.e., order of 100 GeV, especially the muon and electron masses. In the SM, smallness of the charged-lepton masses is just accommodated by taking the Yukawa coupling constants to be $\mathcal{O}(10^{-3})$ and $\mathcal{O}(10^{-5})$ for the muon and electron masses, respectively. In Refs. [18,19], several models have been proposed, where charged-lepton masses are radiatively induced.[2] However, tiny neutrino masses are not explained simultaneously in a given model.

In this paper, we would like to explain the following two questions regarding the lepton masses by extending the radiative seesaw mechanism: (1) why the lepton masses are so small as compared to the electroweak scale, and (2) why there is a large difference between masses of neutrinos and those of the electron or muon. In Ref. [21], we have proposed a new mechanism where Majorana masses of neutrinos and Dirac masses of charged leptons are induced

*hokada@kias.re.kr

†keiyagyu@ncu.edu.tw

[1]There are other types of radiative seesaw models without a DM candidate, e.g., the Zee model [2] and the Zee-Babu model [3].

[2]In Ref. [20], the quark masses and mixing are radiatively induced in a model with two Higgs doublet Higgs fields.

from a different type of dimension-five operator: $\overline{L_L^c} L_L \Delta_0 \Delta_1$ and $\bar{L}_L e_R \Phi \Delta_0$, respectively, where $\Delta_0(\Delta_1)$ is a hypercharge[3] $Y = 0(Y = 1)$ isospin triplet scalar field, and e_R is the right-handed charged-lepton singlet fields. It is known that the magnitude of the vacuum expectation value (VEV) of triplet scalar fields is severely constrained by the electroweak rho parameter; i.e., they have to be smaller than order or 1 GeV. Therefore, for question (1), smallness can be explained by the loop suppression factor if the dimension-five operators are generated via loop levels and the tiny VEVs of triplet scalar fields as well. In addition, question (2) can be described by the difference in the number of triplet VEVs for the generation of masses for neutrinos and charged leptons.

We then have constructed a concrete renormalizable model [21] incorporated the above mechanism, in which both the dimension-five operators are induced at the one-loop level. However, we need rather large Yukawa coupling constants, such as ones greater than about 3, to reproduce the muon mass. The main reason for this problem comes from the too strong suppression by the triplet VEV for the muon mass. Therefore, in this paper, we replace the one-loop induced dimension-five operator $\bar{L}_L e_R \Phi \Delta_0$ by a dimension-seven operator $\bar{L}_L e_R \Phi \chi\chi\chi$ with a SM gauge singlet scalar field χ. We introduce an additional local $U(1)'$ symmetry which is spontaneously broken by the singlet VEV, so that the singlet VEV is expected to be an order of 1 TeV with an order-one $U(1)'$ gauge coupling constant to get a mass of the extra gauge boson to be $\mathcal{O}(1)$ TeV. Under these modifications, we can reproduce the muon mass with $\mathcal{O}(1)$ Yukawa coupling constants.

In our model, additional vectorlike charged leptons play a crucial role in generating the lepton masses. Moreover, the discrepancy in the observed muon anomalous magnetic moment (muon $g-2$) from the prediction in the SM can be compensated by one-loop contributions of the additional charged leptons with the mass of order 1 TeV. We then discuss the collider phenomenology in the favored parameter regions by taking into account the masses of the muon, neutrinos, muon $g-2$, and DM physics.

This paper is organized as follows. In Sec. II, we define our model, and we give the Lagrangian relevant to the generation of the lepton masses. In Sec. III, several observables in the lepton sector are calculated, e.g., masses for the charged leptons and neutrinos, the muon $g-2$, and lepton flavor violating (LFV) processes. Section IV is devoted to study the collider phenomenology of our model. Conclusions and discussions are given in Sec. V. Explicit formulas for the mass matrices for Higgs bosons are given in the Appendix.

[3]The definition of the hypercharge Y is given as $Q = Y + T_3$ with Q and T_3 being the electromagnetic charge and the third component of the isospin.

II. THE MODEL

We propose a radiative lepton mass model where both Dirac charged-lepton (muon and electron) masses and Majorana neutrino masses are generated at the one-loop level. We introduce an extra local $U(1)'$ (spontaneously broken) and a discrete $\mathbb{Z}_2$ (unbroken) symmetry in addition to the SM gauge symmetry. The particle contents and charge assignment are shown in Table I. To avoid tree-level mixing between the Z boson and a new $U(1)'$ gauge boson, we take the $U(1)'$ charge for the doublet Higgs field Φ to be zero.[4] Under the requirement where all the terms given in Eq. (1) are allowed, the $U(1)'$ charges for fields listed in Table I can be written in terms of those for L_L^i, e_R^a, and Δ_0 denoted by x, y, and z, respectively. In order to forbid undesired terms giving tree-level masses for the charged leptons and neutrinos, i.e., $\overline{L_L^{ic}} \Delta_1 L_L^j$ and $\overline{L_L^i} \Phi e_R^a$, $z \neq 0$ and $x - y \neq 0$ must be satisfied, respectively. From the former condition, Δ_0 has to be a complex field. Such a complex $Y = 0$ triplet field has also been introduced in Ref. [22] in a supersymmetric model. Notice here that the condition $x \neq y$ suggests that the $U(1)'$ symmetry cannot be identified as a lepton number symmetry. The scalar fields $\Phi_{3/2}$, η, and S and the vectorlike charged leptons E^α are assigned to be $\mathbb{Z}_2$ odd to enclose the loops in the diagrams for the radiative generation of lepton masses.

Comparing the current model with the previous model, the SM gauge singlet scalar field χ with a nonzero VEV is additionally introduced, and the $Y = 0$ triplet scalar field Δ_0 is extended to be the complex field as mentioned above.[5]

The relevant Lagrangian to the radiative generations of lepton masses is given as follows:

$$\begin{aligned} -\mathcal{L} = {} & M_\alpha \overline{E_R^\alpha} E_L^\alpha + y_\tau^i \overline{L_L^i} \Phi \tau_R + \text{H.c.} \\ & + y_S^{a\alpha} \overline{e_R^a} E_L^\alpha S^* + y_\eta^{i\alpha} \overline{L_L^i} \eta E_R^\alpha + y_{3/2}^{i\alpha} \overline{L_L^{ic}} (i\tau_2) \Phi_{3/2} E_L^\alpha + \text{H.c.} \\ & + \kappa_{e1} \chi^2 S^2 + \kappa_{e2} \eta^\dagger \Phi S^* \chi + \kappa_\nu \text{Tr}(\Delta_1 \cdot \Delta_0)(\Phi_{3/2}^\dagger \cdot \eta) + \text{H.c.}, \end{aligned} \tag{1}$$

where M_α is the mass of the αth vectorlike lepton, and a pair of $\cdot$'s in the κ_ν term denotes the contraction by the Pauli matrices, i.e., $(A \cdot B)(C \cdot D) \equiv \sum_{i=1,2,3} (A\tau^i B)(C\tau^i D)$. We note that the coupling constants $y_\eta^{i\alpha}$, $y_S^{a\alpha}$, and $y_{3/2}^{i\alpha}$ are the arbitrary complex $3 \times \alpha$, $2 \times \alpha$, and $3 \times \alpha$ matrices, respectively. In Fig. 1, Feynman diagrams for the Dirac charged-lepton masses and Majorana neutrino masses are shown. Calculations of these diagrams are performed in the next section.

[4]Although, in general, there is mixing from the gauge kinetic term, we just drop such mixing term by hand.

[5]We can also construct another model without the Δ_0 field by changing the $U(1)'$ charge assignment for fields, in which the dimension-five operator $\overline{L_L^c} L_L \Delta_0 \Delta_1$ for neutrino masses is replaced by $\overline{L_L^c} L_L \Delta_1 \chi$.

TABLE I. The contents of lepton (upper table) and scalar boson (lower table) fields and their charge assignment under $SU(2)_I \times U(1)_Y \times U(1)' \times \mathbb{Z}_2$, where $U(1)'$ is the additional gauge symmetry. The $U(1)'$ charges for L_L^i, e_R^a, and Δ_0 are, respectively, denoted as x, y, and z, and those for all the other fields are expressed in terms of x, y, and z. The index $i(a)$ for $L_L(e_R)$ runs over the first, second, and third (first and second) generations.

Fermions	$L_L^i = (L_L^e, L_L^\mu, L_L^\tau)$	$e_R^a = (e_R, \mu_R)$	τ_R	E_L^α	E_R^α
$SU(2)_I, U(1)_Y$	$\mathbf{2}, -1/2$	$\mathbf{1}, -1$	$\mathbf{1}, -1$	$\mathbf{1}, -1$	$\mathbf{1}, -1$
$U(1)'$	x	y	x	$-x+2y$	$-x+2y$
$\mathbb{Z}_2$	$+$	$+$	$+$	$-$	$-$

Scalar bosons	Φ	Δ_0	Δ_1	η	$\Phi_{3/2}$	S	χ
$SU(2)_I, U(1)_Y$	$\mathbf{2}, 1/2$	$\mathbf{3}, 0$	$\mathbf{3}, 1$	$\mathbf{2}, 1/2$	$\mathbf{2}, 3/2$	$\mathbf{1}, 0$	$\mathbf{1}, 0$
$U(1)'$	0	z	$-(2x+z)$	$2(x-y)$	$-2y$	$y-x$	$x-y$
$\mathbb{Z}_2$	$+$	$+$	$+$	$-$	$-$	$-$	$+$

The scalar potential can be separated into the $\mathbb{Z}_2$-even, $\mathbb{Z}_2$-odd, and interaction parts due to the unbroken $\mathbb{Z}_2$ parity as

$$V = V_{Z_2\text{-even}} + V_{Z_2\text{-odd}} + V_{\text{int}}, \tag{2}$$

where each part is given by

$$\begin{aligned} V_{Z_2\text{-even}} = {} & +m_\Phi^2 \Phi^\dagger\Phi + m_{\Delta_1}^2 \mathrm{Tr}(\Delta_1^\dagger\Delta_1) + m_{\Delta_0}^2 \mathrm{Tr}(\Delta_0^\dagger\Delta_0) + m_\chi^2 \chi^*\chi + \lambda_1(\Phi^\dagger\Phi)^2 + \lambda_2[\mathrm{Tr}(\Delta_1^\dagger\Delta_1)]^2 + \lambda_3 \mathrm{Tr}(\Delta_1^\dagger\Delta_1)^2 \\ & + \lambda_4[\mathrm{Tr}(\Delta_0^\dagger\Delta_0)]^2 + \lambda_5 \mathrm{Tr}(\Delta_0^\dagger\Delta_0)^2 + \lambda_6(\chi^*\chi)^2 + \lambda_7(\Phi^\dagger\Phi)\mathrm{Tr}(\Delta_1^\dagger\Delta_1) + \lambda_8(\Phi^\dagger\cdot\Phi)\mathrm{Tr}(\Delta_1^\dagger\cdot\Delta_1) + \lambda_9(\Phi^\dagger\Phi)\mathrm{Tr}(\Delta_0^\dagger\Delta_0) \\ & + \lambda_{10}(\Phi^\dagger\cdot\Phi)\mathrm{Tr}(\Delta_0^\dagger\cdot\Delta_0) + \lambda_{11}(\Phi^\dagger\Phi)\chi^*\chi + \lambda_{12}\mathrm{Tr}(\Delta_1^\dagger\Delta_1)\chi^*\chi + \lambda_{13}\mathrm{Tr}(\Delta_0^\dagger\Delta_0)\chi^*\chi + \lambda_{14}\mathrm{Tr}(\Delta_1^\dagger\Delta_1)\mathrm{Tr}(\Delta_0^\dagger\Delta_0) \\ & + \lambda_{15}\mathrm{Tr}(\Delta_1^\dagger\Delta_0)\mathrm{Tr}(\Delta_0^\dagger\Delta_1) + \lambda_{16}\mathrm{Tr}(\Delta_1^\dagger\Delta_1\Delta_0^\dagger\Delta_0) + \lambda_0\Phi^T(i\tau_2)\Delta_1^\dagger\Phi\chi + \lambda_0'\Phi^\dagger\Delta_0\Phi\chi + \text{H.c.}, \end{aligned} \tag{3}$$

$$\begin{aligned} V_{Z_2\text{-odd}} = {} & +m_\eta^2\eta^\dagger\eta + m_{3/2}^2\Phi_{3/2}^\dagger\Phi_{3/2} + m_S^2 S^*S + \xi_1(\eta^\dagger\eta)^2 + \xi_2(\Phi_{3/2}^\dagger\Phi_{3/2})^2 + \xi_3(S^*S)^2 + \xi_4(\eta^\dagger\eta)(\Phi_{3/2}^\dagger\Phi_{3/2}) \\ & + \xi_5|\eta^\dagger\Phi_{3/2}|^2 + \xi_6(\eta^\dagger\eta)S^*S, \end{aligned} \tag{4}$$

$$\begin{aligned} V_{\text{int}} = {} & +\kappa_1(\Phi^\dagger\Phi)(\eta^\dagger\eta) + \kappa_2|\Phi^\dagger\eta|^2 + \kappa_3(\Phi^\dagger\Phi)(\Phi_{3/2}^\dagger\Phi_{3/2}) + \kappa_4|\Phi^\dagger\Phi_{3/2}|^2 + \kappa_5(\Phi^\dagger\Phi)S^*S + \kappa_6\mathrm{Tr}(\Delta_1^\dagger\Delta_1)\eta^\dagger\eta \\ & + \kappa_7\mathrm{Tr}(\Delta_1^\dagger\cdot\Delta_1)\eta^\dagger\cdot\eta + \kappa_8\mathrm{Tr}(\Delta_1^\dagger\Delta_1)\Phi_{3/2}^\dagger\Phi_{3/2} + \kappa_9\mathrm{Tr}(\Delta_1^\dagger\cdot\Delta_1)\Phi_{3/2}^\dagger\cdot\Phi_{3/2} + \kappa_{10}\mathrm{Tr}(\Delta_1^\dagger\Delta_1)S^*S + \kappa_{11}\mathrm{Tr}(\Delta_0^\dagger\Delta_0)\eta^\dagger\eta \\ & + \kappa_{12}\mathrm{Tr}(\Delta_0^\dagger\cdot\Delta_0)\eta^\dagger\cdot\eta + \kappa_{13}\mathrm{Tr}(\Delta_0^\dagger\Delta_0)\Phi_{3/2}^\dagger\Phi_{3/2} + \kappa_{14}\mathrm{Tr}(\Delta_0^\dagger\cdot\Delta_0)\Phi_{3/2}^\dagger\cdot\Phi_{3/2} + \kappa_{15}\mathrm{Tr}(\Delta_0^\dagger\Delta_0)S^*S + \kappa_{16}\chi^*\chi\eta^\dagger\eta \\ & + \kappa_{17}\chi^*\chi\Phi_{3/2}^\dagger\Phi_{3/2} + \kappa_{18}\chi^*\chi S^*S + \kappa_{e1}\chi^2S^2 + \kappa_{e2}\eta^\dagger\Phi S^*\chi + \kappa_\nu\mathrm{Tr}(\Delta_1\cdot\Delta_0)(\Phi_{3/2}^\dagger\cdot\eta) + \tilde{\kappa}_\nu\mathrm{Tr}(\Delta_1\Delta_0)(\Phi_{3/2}^\dagger\eta) + \text{H.c.} \end{aligned} \tag{5}$$

The κ_{e1}, κ_{e2}, and κ_ν terms in Eq. (5) already appeared in the Lagrangian in Eq. (1). The λ_0 and λ_0' terms in the last line in Eq. (3) break accidental global $U(1)$ symmetries associated with the phase transformation of triplet scalar bosons, i.e., $\Delta_{0,1} \to e^{i\theta_{0,1}}\Delta_{0,1}$, so that we can avoid the appearance of additional Nambu-Goldstone (NG) bosons.

The scalar fields can be parametrized as

$$\Phi = \begin{bmatrix} \phi^+ \\ \phi^0 \end{bmatrix}, \qquad \eta = \begin{bmatrix} \eta^+ \\ \eta^0 \end{bmatrix}, \qquad \Phi_{3/2} = \begin{bmatrix} \Phi_{3/2}^{++} \\ \Phi_{3/2}^{+} \end{bmatrix}, \qquad \Delta_1 = \begin{bmatrix} \frac{\Delta_1^+}{\sqrt{2}} & \Delta_1^{++} \\ \Delta_1^0 & -\frac{\Delta_1^+}{\sqrt{2}} \end{bmatrix}, \qquad \Delta_0 = \begin{bmatrix} \frac{\Delta_0^0}{\sqrt{2}} & \Delta_0^+ \\ \bar{\Delta}_0^- & -\frac{\Delta_0^0}{\sqrt{2}} \end{bmatrix}. \tag{6}$$

The neutral components of the above fields and the singlet scalar fields can be expressed as

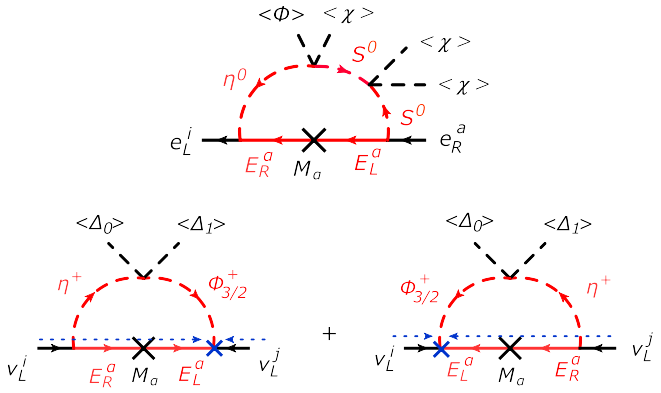

FIG. 1 (color online). Feynman diagrams for the one-loop generation of the charged-lepton masses (upper panel) and neutrino masses (lower panel). The particles indicated by red have the $\mathbb{Z}_2$-odd parity. The blue dotted arrows in the lower diagrams indicate the flow of lepton number, and the blue x shows the lepton number violation with two units.

$$\phi^0=\frac{1}{\sqrt{2}}(\phi_R+v_\phi+i\phi_I),\quad \eta^0=\frac{1}{\sqrt{2}}(\eta_R+i\eta_I),$$
$$\Delta_0^0=\frac{1}{\sqrt{2}}(\Delta_{0R}+v_{\Delta_0}+i\Delta_{0I}),\quad \Delta_1^0=\frac{1}{\sqrt{2}}(\Delta_{1R}+v_{\Delta_1}+i\Delta_{1I}),$$
$$S=\frac{1}{\sqrt{2}}(S_R+iS_I),\quad \chi=\frac{1}{\sqrt{2}}(\chi_R+v_\chi+i\chi_I), \tag{7}$$

where v_ϕ, v_{Δ_0}, v_{Δ_1}, and v_χ are the VEVs of Φ, Δ_0, Δ_1, and χ, respectively. The Fermi constant G_F is given by $v^2\equiv v_\phi^2+2v_{\Delta_1}^2+4v_{\Delta_0}^2=1/(\sqrt{2}G_F)$. Because Δ_0 is the complex field, $\bar{\Delta}_0^+$ does not correspond to $(\Delta_0^-)^*$.

The electroweak rho parameter ρ deviates from unity due to the nonzero value of v_{Δ_0} and v_{Δ_1} at the tree level as

$$\rho=\frac{v^2}{v^2+2v_{\Delta_1}^2-4v_{\Delta_0}^2}. \tag{8}$$

The experimental value of the rho parameter is close to unity so that the triplet VEVs must be much smaller than v as seen in Eq. (8), and the upper limit is typically given as order of 1 GeV.

We then calculate the masses of the $\mathbb{Z}_2$-odd scalar bosons in the Appendix, and we also give details of the discussion for mass matrices for the $\mathbb{Z}_2$-even scalar bosons. The mass terms for the $\mathbb{Z}_2$-odd scalar bosons can be written by

$$V_{\rm mass}=m^2_{\Phi^{++}_{3/2}}\Phi^{++}_{3/2}\Phi^{--}_{3/2}+(\Phi^+_{3/2},\eta^+)M_C^2\begin{pmatrix}\Phi^-_{3/2}\\ \eta^-\end{pmatrix}+\frac{1}{2}(S_I,\eta_I)M_I^2\begin{pmatrix}S_I\\ \eta_I\end{pmatrix}+\frac{1}{2}(S_R,\eta_R)M_R^2\begin{pmatrix}S_R\\ \eta_R\end{pmatrix}, \tag{9}$$

where M_C^2, M_I^2, and M_R^2 are the 2×2 mass matrices for the singly charged, CP-odd, and CP-even scalar boson states, respectively. All the masses of $\mathbb{Z}_2$-odd scalar bosons can be extracted from the potential given in Eqs. (4) and (5). The mass of the doubly charged scalar bosons is calculated by

$$m^2_{\Phi^{++}_{3/2}}=m^2_{3/2}+\frac{1}{2}[\kappa_4 v_\phi^2+\kappa_{18}v_\chi^2+(\kappa_9-\kappa_{10})v_{\Delta_1}^2+\kappa_{14}v_{\Delta_0}^2]. \tag{10}$$

The elements of each mass matrix are obtained as

$$(M_C^2)_{11}=m^2_{3/2}+\frac{1}{2}[(\kappa_3+\kappa_4)v_\phi^2+\kappa_{17}v_\chi^2+(\kappa_8+\kappa_9)v_{\Delta_1}^2+\kappa_{13}v_{\Delta_0}^2], \tag{11a}$$
$$(M_C^2)_{22}=\bar{m}_\eta^2-\frac{1}{2}(\kappa_2 v_\phi^2+\kappa_{16}v_\chi^2+2\kappa_7 v_{\Delta_1}^2), \tag{11b}$$
$$(M_C^2)_{12}=-\frac{\kappa_\nu}{\sqrt{2}}v_{\Delta_1}v_{\Delta_0}, \tag{11c}$$
$$(M_{I,R}^2)_{11}=\bar{m}_S^2\mp\kappa_{e1}v_\chi^2, \tag{11d}$$
$$(M_I^2)_{22}=(M_R^2)_{22}=\bar{m}_\eta^2, \tag{11e}$$
$$(M_{I,R}^2)_{12}=\mp\frac{\kappa_{e2}}{2}v_\phi v_\chi, \tag{11f}$$

where

$$\bar{m}_S^2=m_S^2+\frac{1}{2}(\kappa_5 v_\phi^2+\kappa_{18}v_\chi^2+\kappa_{10}v_{\Delta_1}^2+\kappa_{15}v_{\Delta_0}^2),$$
$$\bar{m}_\eta^2=m_\eta^2+\frac{1}{2}[(\kappa_1+\kappa_2)v_\phi^2+\kappa_{16}v_\chi^2+(\kappa_6+\kappa_7)v_{\Delta_1}^2+\kappa_{11}v_{\Delta_0}^2]. \tag{12}$$

The mass eigenstates for the CP-odd and CP-even scalar states are obtained by introducing the mixing angles as

$$\begin{pmatrix}S_I\\ \eta_I\end{pmatrix}=R(\theta_I)\begin{pmatrix}A_1\\ A_2\end{pmatrix},\quad \begin{pmatrix}S_R\\ \eta_R\end{pmatrix}=R(\theta_R)\begin{pmatrix}H_1\\ H_2\end{pmatrix},\quad \text{with}$$
$$R(\theta)=\begin{pmatrix}\cos\theta & -\sin\theta\\ \sin\theta & \cos\theta\end{pmatrix}. \tag{13}$$

The mass eigenvalues and the mixing angles are given as

$$m^2_{A_{1,2}}=\frac{1}{2}\left[(M_I^2)_{11}+(M_I^2)_{22}\pm\sqrt{[(M_I^2)_{11}-(M_I^2)_{22}]^2+4(M_I^2)_{12}^2}\right], \tag{14a}$$
$$m^2_{H_{1,2}}=\frac{1}{2}\left[(M_R^2)_{11}+(M_R^2)_{22}\pm\sqrt{[(M_R^2)_{11}-(M_R^2)_{22}]^2+4(M_R^2)_{12}^2}\right], \tag{14b}$$

$$\sin 2\theta_I = \frac{2(M_I^2)_{12}}{\sqrt{[(M_I^2)_{11}-(M_I^2)_{22}]^2+4(M_I^2)_{12}^2}} = \frac{2(M_I^2)_{12}}{m_{A_1}^2-m_{A_2}^2}, \tag{14c}$$

$$\sin 2\theta_R = -\frac{2(M_R^2)_{12}}{\sqrt{[(M_R^2)_{11}-(M_R^2)_{22}]^2+4(M_R^2)_{12}^2}} = \frac{2(M_R^2)_{12}}{m_{H_1}^2-m_{H_2}^2}. \tag{14d}$$

We note that the mass difference between H_1 and A_1 and that of H_2 and A_2 are generated only through the κ_{e1} term as seen in Eqs. (11d) and (14d), which is essentially important to obtain the nonzero one-loop generated masses of the charged leptons. The mixing angle for the mass matrix M_C^2 is also given as

$$\sin 2\theta_C = \frac{2(M_C^2)_{12}}{\sqrt{[(M_C^2)_{11}-(M_C^2)_{22}]^2+4(M_C^2)_{12}^2}} \simeq -\frac{\sqrt{2}\kappa_\nu v_{\Delta_1} v_{\Delta_0}}{|m_{\Phi_{3/2}^+}^2 - m_{\eta^+}^2|}, \tag{15}$$

where $m_{\Phi_{3/2}^+}^2 = (M_C^2)_{11}$ and $m_{\eta^+}^2 = (M_C^2)_{22}$. The approximation is valid as long as the triplet VEVs v_{Δ_1} and v_{Δ_0} are quite smaller than v_ϕ and v_χ. It is seen that the mixing angle θ_C is much suppressed by v_{Δ_1} and v_{Δ_0} so that the mass eigenstates for the singly charged scalar bosons are almost the same as the corresponding weak eigenstates $\Phi_{3/2}^\pm$ and $\eta^\pm$. We note that the lightest neutral scalar boson can be a DM candidate.

In our model, there appears an additional neutral gauge boson, a Z' boson, from the $U(1)'$ gauge symmetry. The mass of the Z' boson is given by the VEV of the singlet scalar field v_χ from the kinetic term

$$\mathcal{L}_{\rm kin}^\chi = |D_\mu \chi|^2 = |[\partial_\mu - i g_{Z'}(x-y)]\chi|^2, \tag{16}$$

where $g_{Z'}$ is the $U(1)'$ gauge coupling constant. We then obtain the mass of the Z' boson by[6] $m_{Z'} = g_{Z'}|x-y|v_\chi$. The Z' mass is constrained by the LEP II experiment depending on the $U(1)'$ charge of each field [23,24]. According to Ref. [24], the magnitudes of the vector coupling v_ℓ and the axial vector coupling a_ℓ in the $\ell\bar{\ell}Z'$ vertex defined by

$$\mathcal{L}_{\rm int} = g_{Z'}\bar{\ell}\gamma^\mu(v_\ell - \gamma_5 a_\ell)\ell Z'_\mu \tag{17}$$

are constrained as

$$|v_e| < \frac{\sqrt{\pi} m_{Z'}}{g_{Z'} m_Z} \times 0.012, \qquad |a_\ell| < \frac{\sqrt{\pi} m_{Z'}}{g_{Z'} m_Z} \times 0.018, \tag{18}$$

at the 95% confidence level from the data of $e^+e^- \to e^+e^-$, $\mu^+\mu^-$ and are needed to calculate the one-loop diagrams for the lepton masses discussed in the next section. In our model, v_ℓ and a_ℓ are given from Table I as

$$v_\ell = \frac{1}{2}(x+y), \qquad a_\ell = \frac{1}{2}(x-y). \tag{19}$$

The constraint given in Eq. (18) can be converted into the constraint on v_χ by using Eq. (19) and the mass formula for Z' as

$$v_\chi \gtrsim (2.1\ \text{TeV}) \times \frac{|x+y|}{|x-y|}, \qquad v_\chi \gtrsim 1.4\ \text{TeV}. \tag{20}$$

In the second condition, the dependence of the $U(1)'$ charges is canceled so that v_χ must be larger than 1.4 TeV at least. We take $v_\chi = 3$ TeV in the numerical analysis discussed in the succeeding sections.

III. OBSERVABLES IN THE LEPTON SECTOR

In this section, we calculate mass matrices for neutrinos and charged leptons and new contributions to the muon anomalous magnetic moment. We also discuss the LFV processes in our model. The relevant Lagrangian for the lepton sector is given in Eq. (1) in the previous section.

First, we calculate the mass matrix for the charged leptons, which is composed of the tree-level contribution and the contribution from the one-loop diagram depicted in Fig. 1:

$$M_\ell = M_\ell^{\rm tree} + M_\ell^{\rm loop} = \begin{pmatrix} (M_\ell)_{11}^{\rm loop} & (M_\ell)_{12}^{\rm loop} & (M_\ell)_{13}^{\rm tree} \\ (M_\ell)_{21}^{\rm loop} & (M_\ell)_{22}^{\rm loop} & (M_\ell)_{23}^{\rm tree} \\ (M_\ell)_{31}^{\rm loop} & (M_\ell)_{32}^{\rm loop} & (M_\ell)_{33}^{\rm tree} \end{pmatrix}, \tag{21}$$

where

$$M_\ell^{\rm tree} = \frac{v_\phi}{\sqrt{2}} y_\tau^i, \tag{22}$$

$$M_\ell^{\rm loop} = \sum_\alpha \frac{M_\alpha}{64\pi^2} y_\eta^{i\alpha} y_S^{a\alpha} \left[\sin 2\theta_R F\left(\frac{m_{H_1}^2}{M_\alpha^2}, \frac{m_{H_2}^2}{M_\alpha^2}\right) + \sin 2\theta_I F\left(\frac{m_{A_1}^2}{M_\alpha^2}, \frac{m_{A_2}^2}{M_\alpha^2}\right)\right]. \tag{23}$$

The loop function is given as

$$F(x,y) = \frac{-x\ln x + y\ln y + xy\ln\frac{x}{y}}{(1-x)(1-y)}. \tag{24}$$

We note that the tree-level contribution only gives the third column of M_ℓ, while the one-loop contribution gives the remaining 3×2 part as expressed in the rightmost side in Eq. (21). Thus, both contributions are necessary to get three

[6] The contribution to $m_{Z'}$ from v_{Δ_0} and v_{Δ_1} are neglected.

mass eigenvalues. Notice here that $M_\ell^{\rm loop}$ becomes zero when $m_{H_1} = m_{A_1}$ and $m_{H_2} = m_{A_2}$ are taken, which causes $\sin\theta_R = -\sin\theta_I$ as seen in Eqs. (11f) and (14). Obviously, $M_\ell^{\rm loop}$ also becomes zero in the case of $\theta_R = \theta_I = 0$. Therefore, both κ_{e1} and κ_{e2} are required to be nonzero to obtain nonzero masses for the charged leptons. In the following, we consider the case with $\alpha = 3$. In fact, although $\alpha = 2$ is enough to obtain three nonzero eigenvalues of M_ℓ, that makes M_ℓ to not be a diagonal form,[7] and it causes dangerous LFV processes such as $\mu \to e\gamma$.

Second, the mass matrix for neutrinos is calculated by

$$(M_\nu)_{ij} = \sum_\alpha \frac{M_\alpha}{32\pi^2}(y_\eta^{i\alpha *} y_{3/2}^{j\alpha} + y_\eta^{j\alpha *} y_{3/2}^{i\alpha}) \times \sin 2\theta_C F\left(\frac{m_{H_1^+}^2}{M_\alpha^2}, \frac{m_{H_2^+}^2}{M_\alpha^2}\right). \quad (25)$$

The above mass matrices are diagonalized by introducing the following unitary matrices:

$$U_\ell (M_\ell^\dagger M_\ell) U_\ell^\dagger = {\rm diag}(|m_e|^2, |m_\mu|^2, |m_\tau|^2), \quad (26)$$

$$U_\nu M_\nu U_\nu^T = {\rm diag}(m_{\nu_e}, m_{\nu_\mu}, m_{\nu_\tau}), \quad \text{with} \quad |U_{\rm PMNS}| \equiv |U_\ell^\dagger U_\nu|, \quad (27)$$

where $U_{\rm PMNS}$ is the Pontecorvo-Maki-Nakagawa-Sakata matrix whose elements are given from neutrino oscillation data [25].

We here take the following assumptions for the Yukawa coupling constants as

$$M_1 = M_2 = M_3 = M,$$
$$y_\eta^{i\alpha} = \begin{pmatrix} y_\eta^{11} & y_\eta^{12} & y_\eta^{13} \\ y_\eta^{12} & y_\eta^{22} & y_\eta^{23} \\ y_\eta^{13} & y_\eta^{23} & \frac{y_\eta^{13} y_\eta^{23}}{y_\eta^{12}} \end{pmatrix},$$
$$y_S^{a\alpha} = \begin{pmatrix} y_S^{11} & 0 & -y_S^{11} \\ 0 & y_S^{22} & -y_S^{22} \end{pmatrix}, \qquad y_\tau^1 = y_\tau^2 = 0, \quad (28)$$

where all the Yukawa couplings y_η, y_S, and $y_{3/2}$ are assumed to be real. Under the above assumptions, the mass matrix for the charged leptons is given as the diagonal form by

$$M_\ell = {\rm diag}\left[\tilde{y}_e \tilde{M}_\ell, \tilde{y}_\mu \tilde{M}_\ell, \frac{v_\phi}{\sqrt{2}} y_\tau^3\right], \quad (29)$$

where

$$\tilde{y}_e = (y_\eta^{11} - y_\eta^{12} y_\eta^{13}/y_\eta^{23}) y_S^{11}, \qquad \tilde{y}_\mu = (y_\eta^{22} - y_\eta^{12} y_\eta^{23}/y_\eta^{13}) y_S^{22}, \quad (30)$$

$$\tilde{M}_\ell = \frac{M}{64\pi^2}\left[\sin 2\theta_R F\left(\frac{m_{H_1}^2}{M^2}, \frac{m_{H_2}^2}{M^2}\right) + \sin 2\theta_I F\left(\frac{m_{A_1}^2}{M^2}, \frac{m_{A_2}^2}{M^2}\right)\right]. \quad (31)$$

From Eq. (29), we can naturally explain the muon mass with the order-one coupling $\tilde{y}_\mu$ when $\tilde{M}_\ell$ is given to be order of 0.1 GeV. Such a value of $\tilde{M}_\ell$ can be realized by taking $M = \mathcal{O}(1)$ TeV, $\sin 2\theta_{R,I} = \mathcal{O}(1)$, and $F(x,y) = \mathcal{O}(0.1)$.[8] The important point here is that we need almost the maximal mixing between the inert singlet S and doublet η fields to reproduce the muon mass. That affects the DM physics. Our DM candidate is similar to the property of the isospin inert doublet field due to the maximal mixing. One of the allowed regions of such a DM mass is known as a resonant solution at around $m_h/2$ if the SM-like Higgs boson is the lightest scalar boson among the neutral CP-even neutral bosons, in which the DM candidate can satisfy the observed relic density [26] and the direct detection [27,28]. On the other hand, once the DM mass exceeds the masses of the W and Z bosons, the annihilation cross section to explain the relic density becomes large, e.g., heavier than $\mathcal{O}(500)$ GeV [29]. Here we assume that the DM candidate has a mass at around $m_h/2$ so as to increase the testability of the additional charged leptons E^α which can be important to test our model at collider experiments as discussed in a later section.

Regarding the neutrino masses and mixing, they can be reproduced by taking appropriate values of the coupling constant $y_{3/2}$. The magnitude of the neutrino masses, typically given as $\mathcal{O}(0.1)$ eV, can be obtained in such a way that $\sin 2\theta_C$ is taken to be $\mathcal{O}(10^{-11})$ with $M = \mathcal{O}(1)$ TeV, $y_\eta y_{3/2} = \mathcal{O}(1)$, and $F = \mathcal{O}(1)$. Such a small mixing angle θ_C can be naturally explained by the smallness of v_{Δ_0} and v_{Δ_1}. When the product of the triplet VEVs $v_{\Delta_0} \times v_{\Delta_1}$ is taken to be order of $(1\ {\rm MeV})^2$ with $\kappa_\nu = \mathcal{O}(1)$, we obtain $\mathcal{O}(10^{-11})$ of the mixing angle θ_C.

The muon anomalous magnetic moment has been measured at Brookhaven National Laboratory. The current average of the experimental results is given by [30]

$$a_\mu^{\rm exp} = 11659208.0(6.3) \times 10^{-10},$$

which has a discrepancy from the SM prediction by 3.2σ [31] to 4.1σ [32] as

[7] Even in the case of $\alpha = 2$, we can obtain a diagonal form of M_ℓ with three nonzero eigenvalues by taking $y_\eta^{3\alpha *} = 0$. However, in that case, it is difficult to reproduce the neutrino mixing.

[8] To reproduce the electron mass, we need to take the ratio of the coupling constants $\tilde{y}_e/\tilde{y}_\mu$ to be $m_e/m_\mu \simeq 5 \times 10^{-3}$.

$$\Delta a_\mu = a_\mu^{\rm exp} - a_\mu^{\rm SM} = (29.0 \pm 9.0 \quad \text{to} \quad 33.5 \pm 8.2) \times 10^{-10}. \tag{32}$$

In our model, the vectorlike charged leptons and $\mathbb{Z}_2$-odd scalar bosons can contribute to the $\ell_a \to \ell_b \gamma$ processes as shown in Fig. 2. The amplitude for these processes is calculated by

$$\Delta a_{ab} \simeq \sum_{\alpha=1}^{3} \frac{m_\mu}{64\pi^2 M_\alpha} (y_S^{a\alpha} y_\eta^{b\alpha} + y_S^{b\alpha} y_\eta^{a\alpha}) \left[\sin 2\theta_R G\left(\frac{m_{H_1}^2}{M_\alpha^2}, \frac{m_{H_2}^2}{M_\alpha^2}\right) + \sin 2\theta_I G\left(\frac{m_{A_1}^2}{M_\alpha^2}, \frac{m_{A_2}^2}{M_\alpha^2}\right) \right], \tag{33}$$

$$\text{with} \quad G(x,y) = \frac{1 - 4x + 3x^2 - 2x^2 \ln x}{2(1-x)^3} - \frac{1 - 4y + 3y^2 - 2y^2 \ln y}{2(1-y)^3}, \tag{34}$$

where terms proportional to $(y_S^{a\alpha})^2$ and $(y_\eta^{a\alpha})^2$ and the $\Phi_{3/2}^{\pm\pm}$ loop contributions are neglected because they are suppressed by the factor of m_μ/M_α compared to Eq. (33). By taking the same assumptions given in Eq. (28), we obtain

$$\Delta a_{ab} = 2\left(\frac{m_\mu}{M^2}\right) \times \mathcal{R} \times (M_\ell)_{ab}, \tag{35}$$

where

$$\mathcal{R} \equiv \frac{\sin 2\theta_R G\left(\frac{m_{H_1}^2}{M^2}, \frac{m_{H_2}^2}{M^2}\right) + \sin 2\theta_I G\left(\frac{m_{A_1}^2}{M^2}, \frac{m_{A_2}^2}{M^2}\right)}{\sin 2\theta_R F\left(\frac{m_{H_1}^2}{M^2}, \frac{m_{H_2}^2}{M^2}\right) + \sin 2\theta_I F\left(\frac{m_{A_1}^2}{M^2}, \frac{m_{A_2}^2}{M^2}\right)}. \tag{36}$$

The contribution to the muon $g-2$ is given by $\Delta a_{\mu\mu} \equiv \Delta a_\mu$. From Eq. (37), we get the following simple formula:

$$\Delta a_\mu = \text{sign}[(M_\ell)_{\mu\mu}] \times 2\left(\frac{m_\mu}{M}\right)^2 \times \mathcal{R}. \tag{37}$$

We note that there is no LFV contribution under the assumption in Eq. (28) because the matrix Δa_{ab} has a diagonal form.

In the following, we show numerical calculations for $\tilde{M}_\ell$ and Δa_μ given in Eqs. (31) and (37) with $\bar{m}_S^2 = \bar{m}_\eta^2 (\equiv \bar{m}^2)$ for simplicity. In that case, the masses of neutral $\mathbb{Z}_2$-odd scalar bosons and their mixing angels are given by

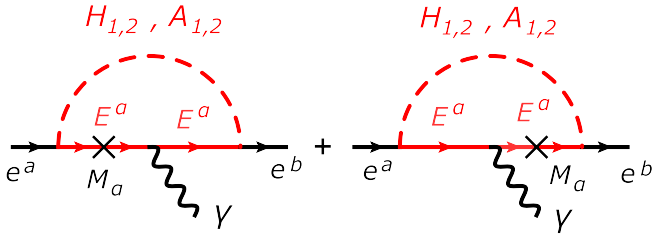

FIG. 2 (color online). Dominant contributions to the $\ell_a \to \ell_b \gamma$ processes. The $\Phi_{3/2}^{\pm\pm}$ loop contribution is neglected because of the suppression by m_μ/M_α as compared to the dominant contributions.

$$\begin{aligned} m_{H_{1,2}}^2 &= \bar{m}^2 + \frac{v_\chi^2}{2}\left(\kappa_{e1} \pm \sqrt{\kappa_{e1}^2 + \kappa_{e2}^2 v^2/v_\chi^2}\right), \\ m_{A_{1,2}}^2 &= \bar{m}^2 + \frac{v_\chi^2}{2}\left(-\kappa_{e1} \pm \sqrt{\kappa_{e1}^2 + \kappa_{e2}^2 v^2/v_\chi^2}\right), \\ \sin 2\theta_R &= -\sin 2\theta_I = \frac{v}{v_\chi} \frac{\kappa_{e2}}{\sqrt{\kappa_{e1}^2 + \kappa_{e2}^2 v^2/v_\chi^2}}. \end{aligned} \tag{38}$$

When κ_{e1} is taken to be a positive value, the mass hierarchy is determined by $m_{H_1} > m_{A_1} > m_{H_2} > m_{A_2}$. Therefore, A_2 is the lightest neutral Z_2-odd particle, and it corresponds to the DM candidate. We discuss the case with $\kappa_{e1} > 0$ in the following calculations. As already explained above, the mass of the DM candidate should be taken as half the Higgs boson mass so that we take $m_{A_2} = 63$ GeV. Instead of fixing the physical masses of scalar bosons and mixing angles, we choose κ_{e1}, κ_{e2}, $v_\chi (= 3$ TeV), $m_{A_2} (= 63$ GeV) as the input parameters. In terms of these input variables, we can rewrite Eq. (38) by

$$\begin{aligned} m_{H_1}^2 &= m_{A_2}^2 + v_\chi^2\left(\kappa_{e1} + \sqrt{\kappa_{e1}^2 + \kappa_{e2}^2 v^2/v_\chi^2}\right), \\ m_{H_2}^2 &= m_{A_2}^2 + v_\chi^2 \kappa_{e1}, \\ m_{A_1}^2 &= m_{A_2}^2 + v_\chi^2 \sqrt{\kappa_{e1}^2 + \kappa_{e2}^2 v^2/v_\chi^2}. \end{aligned} \tag{39}$$

In Fig. 3, we show the contours of $\tilde{M}_\ell$ and $\Delta a_\mu \times 10^9$ denoted by black and red curves, respectively, on the κ_{e1}-κ_{e2} plane. The mass of the vectorlike leptons M is taken to be 1500 GeV (upper-left panel), 1000 GeV (upper-right panel), 750 GeV (lower-left panel), and 500 GeV (lower-right panel). It is seen that the M dependence of $\tilde{M}_\ell$ is weak, while that of Δa_μ is quite strong because of the $(m_\mu/M)^2$ factor in Eq. (37). When we take $\kappa_{e2} \gtrsim 0.01$ ($\kappa_{e2} \gtrsim 0.1$ and $\kappa_{e1} \gtrsim 0.03$), $\tilde{M}_\ell > 0.01(0.1)$ GeV can be obtained. Regarding Δa_μ, when $M = 1500$ GeV and 500 GeV is taken, the value of Δa_μ becomes smaller than about 2.0×10^{-9} and larger than about 1.0×10^{-8}, respectively, in the regions of κ_{e1} and κ_{e2} shown in Fig. 3. In the case of $M = 1000(750)$ GeV, $\Delta a_\mu \simeq 3.0 \times 10^{-9}$ is obtained when we take $\kappa_{e1} = 0.008 - 0.02$ ($\kappa_{e1} = 0.001 - 0.002$ and $\kappa_{e2} \lesssim 0.04$). Therefore, M to be

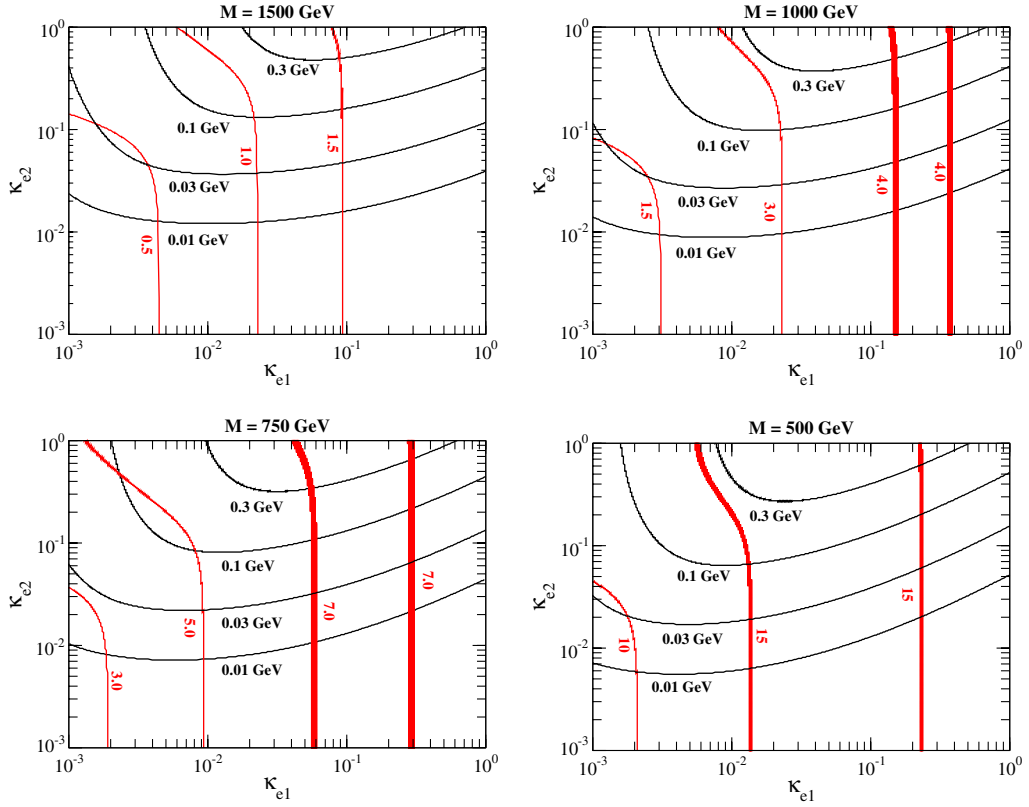

FIG. 3 (color online). Contour plots for $\tilde{M}_\ell$ (black curves) and $\Delta a_\mu \times 10^9$ (red curves) on the κ_{e1}–κ_{e2} plane. We take $M = 1500$, 1000, 750, and 500 GeV in the upper-left, upper-right, lower-left, and lower-right panels, respectively.

around 1 TeV is favored by the measurement of the muon $g-2$.

In Fig. 4, we show the contours of $\Delta a_\mu \times 10^9$ on the $\kappa_{e1} - M$ plane for the fixed values of κ_{e2} to be 0.1 (left panel) and 1 (right panel). We can expect that the result does not change in the case with values of κ_{e2} smaller than 0.1 as seen in Fig. 3. In both cases with $\kappa_{e2} = 0.1$ and 1, when M is taken to be around 1000 GeV, we can get $\Delta a_\mu \simeq 3.0 \times 10^{-9}$. When M is taken to be smaller (larger) than about 700 (2000) GeV, Δa_μ becomes larger (smaller) than $5.0(1.0) \times 10^{-9}$, which are outside of the $2(\sigma)$ error of the measured Δa_μ.

In Fig. 5, we show the contour plots for the output values of m_{H_1} (upper left), m_{H_2} (upper right), m_{A_1} (lower left), and $\bar{m}$ (lower right) on the $\kappa_{e1} - \kappa_{e\tilde{2}}$ plane. The red, blue, and green shaded regions satisfy $\tilde{M}_\ell > 0.03$ GeV and $2.0 \times 10^{-9} < \Delta a_\mu < 4.2 \times 10^{-9}$ in the case of $M = 1250$, 1000, and 750 GeV, respectively. The condition for Δa_μ corresponds to the requirement where the prediction of Δa_μ is inside the $1(\sigma)$ error from the measurement. We can see that

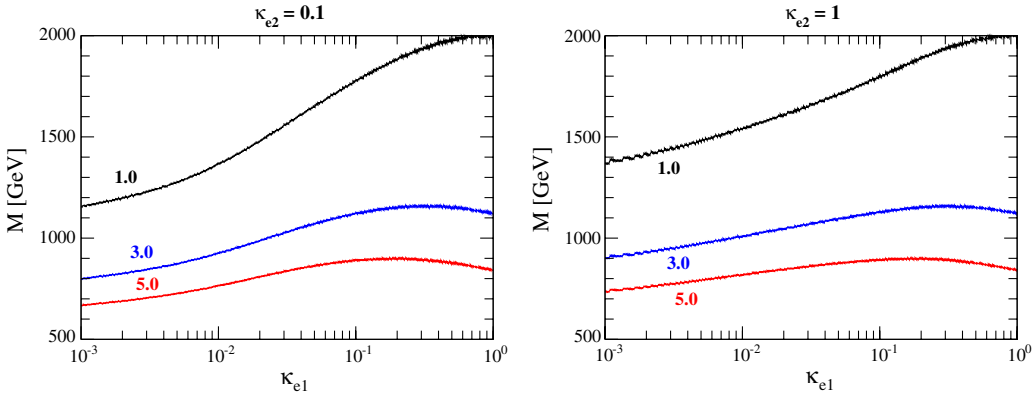

FIG. 4 (color online). Contour plots for $\Delta a_\mu \times 10^9$ on the κ_{e1}–M plane. The value of κ_{e2} is fixed to be 0.1 and 1 in the left and right panels, respectively.

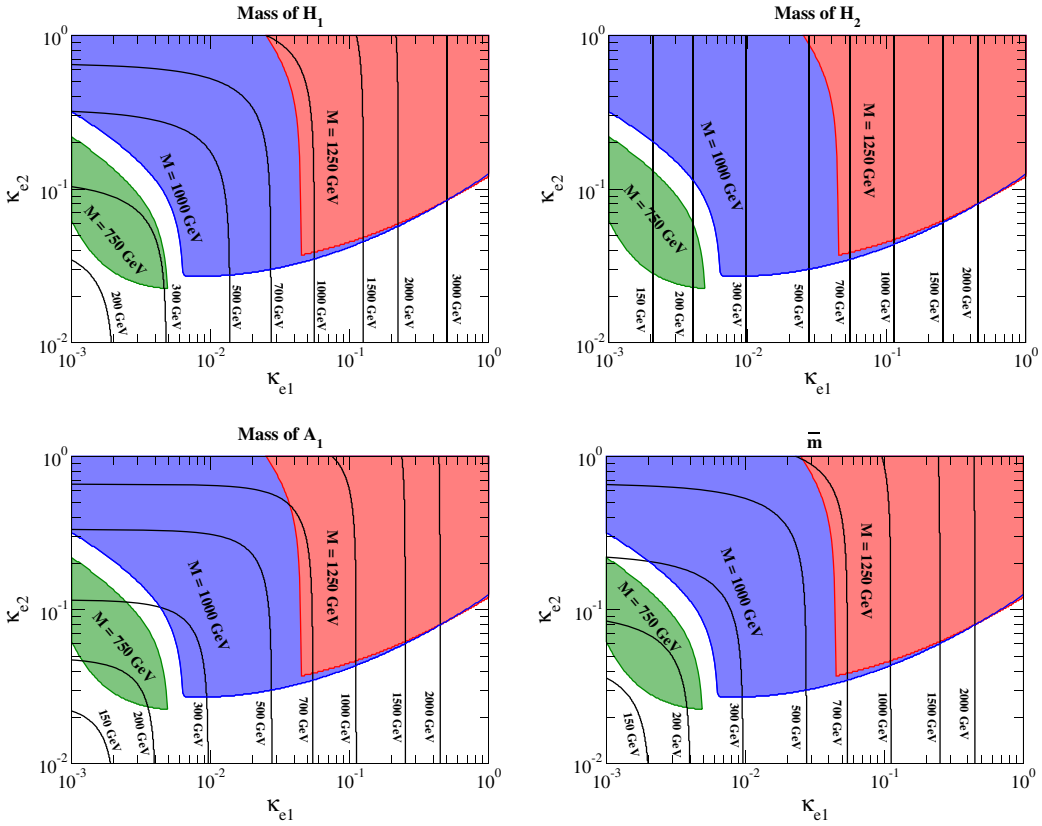

FIG. 5 (color online). Contour plots for m_{H_1} (upper-left panel), m_{H_2} (upper-right panel), m_{A_1} (lower-left panel), and $\bar{m}$ (lower-right panel) on the κ_{e1}–κ_{e2} plane. The red and blue shaded regions satisfy $\tilde{M}_\ell > 0.03$ GeV, $2.0 \times 10^{-9} < \Delta a_\mu < 4.2 \times 10^{-9}$.

the shaded regions are shifted from the lower-left region to the upper-right region on the $\kappa_{e1} - \kappa_{e2}$ plane when the value of M is changed from 750 to 1250 GeV. That is because the prediction of Δa_μ is getting smaller as M is increased so to compensate the suppression by M, we need larger values of κ_{e1} and κ_{e2}. In the case of $M = 750$ GeV, the case with $220 \lesssim m_{H_1} \lesssim 400$ GeV, $180 \lesssim m_{A_1} \lesssim 400$ GeV, and $110 \lesssim m_{H_2} \lesssim 220$ GeV is favored by $g-2$ data and natural explanation for the muon mass by means of $\tilde{M}_\ell > 0.03$ GeV. Similarly, in the case of $M = 1000$ GeV, the case of $m_{H_1} \gtrsim 350$ GeV, $m_{A_1} \gtrsim 250$ GeV, and $m_{A_1} \gtrsim 250$ GeV is favored.

IV. COLLIDER PHENOMENOLOGY

In this section, we discuss the collider phenomenology in our model. As seen in the Feynman diagrams shown in Fig. 1, the vectorlike leptons $E_\alpha^\pm (\alpha = 1, 2, 3)$ play an essential role to generate the masses of both charged leptons and neutrinos. Therefore, the detection of $E_\alpha^\pm$ is important to test our model. In the following analysis, we take the assumptions given in Eq. (28) and

$$y_\eta^{ij} = \bar{y}_\eta, \quad \text{for } i \neq j, \qquad y_\eta^{11} = y_\eta^{22} = 0. \tag{40}$$

The decay of $E_\alpha^\pm$ depends on the mass spectrum for the $\mathbb{Z}_2$-odd particles, some of which can be determined by taking into account the muon mass and Δa_μ as seen in Fig. 5. As examples, we consider the benchmark points listed in Table II. Among the $\mathbb{Z}_2$-odd particles, the mass of $\Phi_{3/2}^{\pm\pm}$ is not determined from experimental data. We can then consider the two cases: (1) $M < m_{\Phi_{3/2}^{++}}$ and (2) $M > m_{\Phi_{3/2}^{++}}$. In case (1), $E_\alpha^\pm$ can decay into $\ell^\pm \varphi^0$ ($\ell = e, \mu$, and τ) and $\eta^\pm \nu$, where φ^0 denotes the neutral $\mathbb{Z}_2$-odd scalar boson (H_1, H_2, A_1, and A_2). On the other hand, in case (2), $E_\alpha^\pm$ can decay into $\Phi_{3/2}^{\pm\pm} \ell^\mp$ and $\Phi_{3/2}^\pm \nu$ via the $y_{3/2}$ coupling in addition to the decay modes listed above.

TABLE II. Benchmark input parameters and corresponding outputs. The masses in the outputs are calculated by using Eq. (39).

	Input parameters				Outputs					
	M	m_{A_2}	κ_{e1}	κ_{e2}	m_{H_1}	m_{A_1}	m_{H_2}	$\bar{m}$	$\tilde{M}_\ell$	Δa_μ
Benchmark I	750 GeV	63 GeV	0.001	−0.1	295 GeV	279 GeV	113 GeV	213 GeV	0.036 GeV	3.6×10^{-9}
Benchmark II	1000 GeV	63 GeV	0.03	−0.1	744 GeV	533 GeV	523 GeV	528 GeV	0.097 GeV	3.2×10^{-9}

We focus on case (1) in the following, in which the decay of $E_\alpha^\pm$ becomes more sensitive to the structure of Yukawa interactions related to the generation of the charged-lepton masses. The sum of decay rates of $E_\alpha^\pm$ defined by $\Gamma(E \to X) \equiv \sum_\alpha \Gamma(E_\alpha \to X)$ are calculated as

$$\Gamma(E^\pm \to e^\pm \varphi_i^0) = \frac{M}{32\pi} \bar{y}_\eta^2 c_{\eta_i}^2 \left(1 - \frac{m_{\varphi_i}^2}{M^2}\right)^2, \quad (41a)$$

$$\Gamma(E^\pm \to \tau^\pm \varphi_i^0) = \frac{3M}{64\pi} \bar{y}_\eta^2 c_{\eta_i}^2 \left(1 - \frac{m_{\varphi_i}^2}{M^2}\right)^2, \quad (41b)$$

$$\Gamma(E^\pm \to \mu^\pm \varphi_i^0) = \frac{M}{32\pi} [\bar{y}_\eta^2 c_{\eta_i}^2 + (y_S^{22})^2 c_{S_i}^2] \left(1 - \frac{m_{\varphi_i}^2}{M^2}\right)^2, \quad (41c)$$

$$\Gamma(E^\pm \to \eta^\pm \nu) = \frac{7M}{64\pi} \bar{y}_\eta^2 \left(1 - \frac{m_{\eta^+}^2}{M^2}\right)^2, \quad (41d)$$

where

$$\varphi_i^0 = (H_1, H_2, A_1, A_2), \quad c_{\eta_i} = (\sin\theta_R, \cos\theta_R, \sin\theta_I, \cos\theta_I),$$
$$c_{S_i} = (\cos\theta_R, \sin\theta_R, \cos\theta_I, \sin\theta_I), \quad \text{for } (i = 1,2,3,4). \quad (42)$$

For the $E^\pm \to \eta^\pm \nu$ mode, final states with ν_e, ν_μ, and ν_τ are summed. The decay rates can be described by the ratio of the two Yukawa couplings $r \equiv y_S^{22}/\bar{y}_\eta$ instead of y_S^{22} and $\bar{y}_\eta$. From Eqs. (29) and (40), the product $y_S^{22} \times \bar{y}_\eta$ has to be fixed by the muon mass, i.e., $y_S^{22} \times \bar{y}_\eta \simeq 2.94(1.09)$ in Benchmark I (II). Therefore, each of the Yukawa couplings is determined by $y_S^{22} = \sqrt{2.94r}(\sqrt{1.09r})$ and $\bar{y}_\eta = \sqrt{2.94/r}(\sqrt{1.09/r})$ in Benchmark I (Benchmark II). We note that H_1 and $H_2(A_1)$ can further decay into $A_2 Z^{(*)}(H_2 Z^{(*)})$, and $\eta^\pm$ can decay into $W^{\pm(*)} A_2$.

In Fig. 6, we show the decay branching fraction of E^+ as a function of the ratio r. The branching ratios for the channel with a neutral $\mathbb{Z}_2$-odd scalar boson in the final state are summed. The results in Benchmark I and Benchmark II are shown as the solid and dashed curves, respectively. From the requirement of perturbativity, i.e., $y_S^{22}, \bar{y}_\eta < 2\sqrt{\pi}$, we can find the lower and upper limits on r. The regions between the two solid (dashed) vertical lines are allowed by perturbativity in Benchmark I (II). We can see that in the large r region, only the branching fraction of the $\mu^+\varphi^0$ mode increases as compared to all the other channels, because only the $E^\pm \mu^\mp \varphi^0$ vertex is enhanced by the large y_S^{22}. Therefore, an excess in the muon plus missing transverse momentum event can be a probe of the existence of $E^\pm$. However, such an excess can also be realized in a supersymmetric model, e.g., from the smuon decay into the muon and neutralino. We then have to measure signals

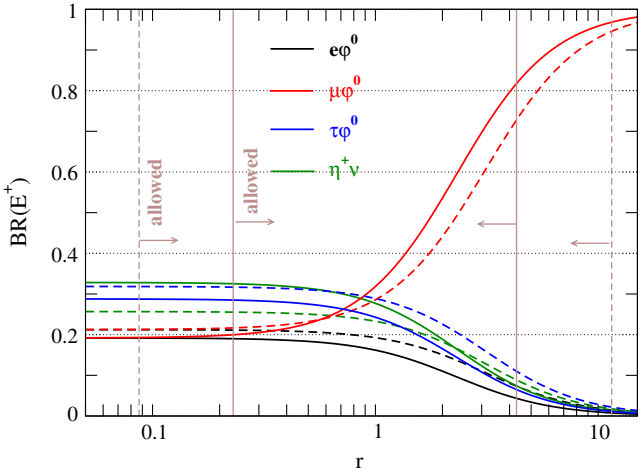

FIG. 6 (color online). Branching fractions of E^+ as a function of the ratio $r \equiv y_S^{22}/\bar{y}_\eta$. The mass of $\eta^\pm$ is taken to be $\bar{m}$. The solid and dashed curves are, respectively, the results in Benchmark I and Benchmark II listed in Table II. $\ell^+\varphi^0(\ell = e, \mu, \tau)$ denotes the sum of all the possible modes with a neutral $\mathbb{Z}_2$-odd scalar boson φ^0. The region between the solid (dashed) vertical lines is allowed from the requirement of perturbativity, i.e., y_S^{22}, $\bar{y}_\eta < 2\sqrt{\pi}$ in Benchmark I (II).

other than that of $E^\pm$, such as the doubly charged scalar bosons $\Phi_{3/2}^{\pm\pm}$, to test our model.

We, thus, consider signatures of $\Phi_{3/2}^{\pm\pm}$ at the LHC. In case (1), the same-sign dilepton plus missing energy event from the decay of $\Phi_{3/2}^{++}$ as shown in Fig. 7 is expected at the LHC. When we consider the case with $r \gg 1$, one of the charged leptons in the final state is more likely to be muon. This signature with the $\mu^+\ell^+$ final state is important to discriminate our model from the other models with doubly charged scalar bosons. We note that the sum of the production cross section for the $pp \to \gamma^*/Z^* \to \Phi_{3/2}^{++}\Phi_{3/2}^{--}$ and $pp \to W^{+*} \to \Phi_{3/2}^{++}\Phi_{3/2}^{-}$ processes at the LHC with the 14 TeV energy is calculated about 0.21, 0.11, and 0.059 fb in the cases of $m_{\Phi^{++}} = 800$, 900, and 1000 GeV, respectively, with taking the mass of $\Phi_{3/2}^{-}$ to be the same as that of $\Phi_{3/2}^{++}$. For the calculation of the above cross sections, we use CALCHEP [33] and CTEQ61 for the parton distribution function.

Finally, we comment on signatures of another pair of doubly charged scalar bosons $\Delta_1^{\pm\pm}$ from the isospin triplet

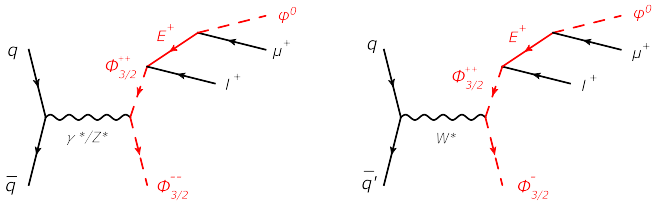

FIG. 7 (color online). Signal processes from $\Phi_{3/2}^{++}$ at the LHC.

field. The tree-level Yukawa interaction for $\Delta_1^{\pm\pm}$ is forbidden by the $U(1)'$ symmetry so that $\Delta_1^{\pm\pm}$ cannot decay into the same-sign dilepton unlike the minimal Higgs triplet model (HTM) [34]. Thus, the main decay mode of $\Delta_1^{\pm\pm}$ is the same-sign diboson; i.e., $\Delta_1^{\pm\pm} \to W^\pm W^\pm$ as long as $\Delta_1^{\pm\pm}$ are the lightest of all the other component fields in Δ_1. Such a decay mode can appear in the HTM with the case of a rather large triplet VEV, i.e., larger than about 1 MeV. The collider phenomenology for the diboson decay scenario had been discussed in Refs. [35,36]. In Ref. [36], by using the LHC data with the collision energy of 7 TeV and integrated luminosity of 4.7 fb^{-1}, the lower mass bound for the doubly charged scalar bosons has been found to be about 60 GeV.

V. CONCLUSIONS AND DISCUSSIONS

We have modified our previous model in Ref. [21] with the one-loop generation of masses for neutrinos, muon, and electron. The masses of a muon and electron are induced by the $\bar{L}_L e_R \Phi \chi\chi\chi$ operator, and those of neutrinos are generated from the $\overline{L_L^c} L_L \Delta_0 \Delta_1$ operator. The doublet VEV v_ϕ and singlet VEV v_χ are, respectively, determined by the Fermi constant G_F and the Z' mass, where the latter VEV has to be above 1 TeV from the constraint from the LEP II experiment. On the other hand, the triplet VEVs must be smaller than about 1 GeV due to the constraint from the electroweak rho parameter. Therefore, the mass hierarchy between neutrinos and charged leptons can be naturally described by the suppression of the triplet VEVs for the neutrino masses with $\mathcal{O}(1)$ Yukawa coupling constants y_S^{22} and $\bar{y}_\eta$.

In our model, the lightest $\mathbb{Z}_2$-odd neutral scalar boson can be a DM candidate, and A_2 corresponds to it when κ_{e1} is taken to be a positive value. The mass of DM is set to be $m_h/2$ in order to satisfy the relic density and the constraint from the direct detection.

Under the assumptions given in Eq. (28) and the requirement from the DM physics, we have calculated the muon $g-2$ and $\tilde{M}_\ell$. We have found that the mass of vectorlike charged leptons $E_\alpha^\pm$ to be around 1 TeV is favored by taking into account the above observables as seen in Fig. 5.

We have studied the decay property of $E_\alpha^\pm$ whose decay branching fractions are shown in Fig. 6 with the two benchmark parameter sets with $M < m_{\Phi_{3/2}^{++}}$. We have found that $E_\alpha^\pm$ can mainly decay into a muon plus neutral $\mathbb{Z}_2$-odd scalar bosons. We also have discussed the signature from doubly charged scalar bosons $\Phi_{3/2}^{\pm\pm}$ and $\Delta_1^{\pm\pm}$.

ACKNOWLEDGMENTS

The authors would like to thank Hiroaki Sugiyama for a useful comment on the model building. K. Y. was supported in part by the National Science Council of R. O. C. under Grant No. NSC-101-2811-M-008-014.

APPENDIX: HIGGS SECTOR WITH THE $\mathbb{Z}_2$ EVEN PART

In this appendix, we give the mass formulas for the $\mathbb{Z}_2$-even Higgs bosons in which we neglect the terms proportional to $v_{\Delta_1}^2$, $v_{\Delta_0}^2$, and $v_{\Delta_0} v_{\Delta_1}$.

From the tadpole conditions, the scalar invariant mass parameters m_Φ^2, m_χ^2, $m_{\Delta_1}^2$, and $m_{\Delta_0}^2$ can be rewritten by

$$
\begin{aligned}
m_\Phi^2 &\simeq \lambda_0 v_{\Delta_1} v_\chi + \frac{\lambda_0'}{\sqrt{2}} v_{\Delta_0} v_\chi - \lambda_1 v_\phi^2 - \frac{\lambda_{12}}{2} v_\chi^2, \\
m_\chi^2 &\simeq \frac{1}{2}\left(\lambda_0 \frac{v_{\Delta_1}}{v_\chi} + \frac{\lambda_0'}{\sqrt{2}} \frac{v_{\Delta_0}}{v_\chi} - \lambda_{11}\right) v_\phi^2 - \lambda_6 v_\chi^2, \\
m_{\Delta_0}^2 &\simeq \frac{1}{2}\left(\frac{\lambda_0' v_\chi}{\sqrt{2} v_{\Delta_0}} - \lambda_9\right) v_\phi^2 - \frac{\lambda_{13}}{2} v_\chi^2, \\
m_{\Delta_1}^2 &\simeq \frac{1}{2}\left(\lambda_0 \frac{v_\chi}{v_{\Delta_1}} - \bar{\lambda}\right) v_\phi^2 - \frac{\lambda_{12}}{2} v_\chi^2,
\end{aligned}
\tag{A1}
$$

where $\bar{\lambda} \equiv \lambda_7 + \lambda_8$.

There are one pair of doubly charged states, four pairs of singly charged states, and four CP-odd and four CP-even states. First, the mass of the doubly charged Higgs boson $\Delta^{\pm\pm}$ is calculated as

$$
m_{\Delta_1^{++}}^2 \simeq \left(\frac{\lambda_0}{2} \frac{v_\chi}{v_{\Delta_1}} - \lambda_8\right) v_\phi^2. \tag{A2}
$$

Second, we discuss the masses of the singly charged scalar states. Because one of four pairs corresponds to the NG boson state which are absorbed into the longitudinal component of the W boson, we can obtain the block diagonal form of the matrix, in which the NG mode is separated into the physical singly charged scalar bosons. When we define the mass matrix for the singly charged state in the basis of $(\phi^+, \Delta_1^+, \Delta_0^+, \bar{\Delta}_0^+)$ with $\bar{\Delta}_0^+ = \bar{\Delta}_0^{-*}$, it can be given as

$$
O_C^T \bar{M}_C^2 O_C \simeq \begin{bmatrix}
0 & 0 & 0 & 0 \\
 & \frac{\sqrt{2}\lambda_0'}{4} \frac{v_\phi^2 v_\chi}{v_{\Delta_0}} & 0 & \frac{\lambda_{10}}{2} v_\phi^2 \\
 & & \frac{1}{2}\left(\frac{v_\chi}{v_{\Delta_1}} \lambda_0 - \lambda_8\right) v_\phi^2 & -\lambda_0' v_{\Delta_1} v_\chi \\
 & & & \frac{\lambda_0'}{2\sqrt{2}} \frac{v_\phi^2 v_\chi}{v_{\Delta_0}}
\end{bmatrix}, \tag{A3}
$$

where

$$O_C \simeq \begin{bmatrix} -1 & 0 & \frac{\sqrt{2}v_{\Delta_1}}{v_\phi} & -\frac{2v_{\Delta_1}}{v_\phi} \\ -\frac{\sqrt{2}v_{\Delta_1}}{v_\phi} & 0 & -1 & 0 \\ \frac{\sqrt{2}v_{\Delta_0}}{v_\phi} & \frac{1}{\sqrt{2}} & 0 & -\frac{1}{\sqrt{2}} \\ \frac{\sqrt{2}v_{\Delta_0}}{v_\phi} & -\frac{1}{\sqrt{2}} & 0 & -\frac{1}{\sqrt{2}} \end{bmatrix}. \tag{A4}$$

Third, two of the four CP-odd states correspond to the NG bosons which are absorbed by the longitudinal component of the Z boson and additional neutral gauge boson from the $U(1)'$ symmetry. Therefore, the mass matrix for the CP-odd states in the basis of $(\phi_I, \chi_I, \Delta_{1I}, \Delta_{0I})$ can be expressed by the block diagonal form with a nonzero 2×2 submatrix as

$$O_I^T \bar{M}_I^2 O_I \simeq \begin{bmatrix} 0 & 0 & 0 & 0 \\ 0 & 0 & 0 & 0 \\ & & \frac{\lambda_0'}{2\sqrt{2}}\frac{v_\phi^2 v_\chi}{v_{\Delta_0}} & \lambda_0 v_\phi v_{\Delta 0} \\ & & & \frac{\lambda_0}{2}\frac{v_\phi^2 v_\chi}{v_{\Delta_1}} \end{bmatrix}, \tag{A5}$$

where

$$O_I \simeq \begin{bmatrix} \frac{1}{\sqrt{2}} r_+ & -\frac{1}{\sqrt{2}} r_- & 0 & \frac{2v_{\Delta_1}}{v_\phi} \\ -\frac{\sqrt{2}}{r_+}\frac{v_\chi}{\bar{v}} & -\frac{\sqrt{2}}{r_-}\frac{v_\chi}{\bar{v}} & \frac{v_{\Delta_0}}{v_\chi} & \frac{v_{\Delta_1}}{v_\chi} \\ \frac{\sqrt{2}}{r_+}\frac{v_{\Delta_1}}{v_\phi} & -\frac{\sqrt{2}}{r_-}\frac{v_{\Delta_1}}{v_\phi} & 0 & -1 \\ \frac{\sqrt{2}}{r_+}\frac{v_{\Delta_0}}{\bar{v}} & -\frac{\sqrt{2}}{r_-}\frac{v_{\Delta_0}}{\bar{v}} & 1 & 0 \end{bmatrix}, \tag{A6}$$

with $r_\pm \equiv \sqrt{1 \pm 1/\sqrt{1 + 4v_\chi^2/v_\phi^2}}$.

Finally, the mass matrix for the CP-even states in the basis of $(\phi_R, \chi_R, \Delta_{1R}, \Delta_{0R})$ is given by

$$\bar{M}_R^2 \simeq \begin{bmatrix} 2\lambda_1 v_\phi^2 & \left(\lambda_{11} v_\chi - \lambda_0 v_{\Delta_1} - \frac{\lambda_0'}{\sqrt{2}} v_{\Delta_0}\right) v_\phi & [-\lambda_0 v_\chi + (\lambda_7 + \lambda_8) v_{\Delta_1}] v_\phi & \left(-\frac{\lambda_0'}{\sqrt{2}} v_\chi + \lambda_9 v_{\Delta_0}\right) v_\phi \\ & \frac{1}{2}\left(4\lambda_6 v_\chi^2 + \lambda_0 \frac{v_{\Delta_1} v_\phi^2}{v_\chi} + \frac{\lambda_0'}{\sqrt{2}} \frac{v_{\Delta_0} v_\phi^2}{v_\chi}\right) & \lambda_{12} v_\chi v_{\Delta_1} - \frac{\lambda_0}{2} v_\phi^2 & \lambda_{13} v_\chi v_{\Delta_0} - \frac{\lambda_0'}{2\sqrt{2}} v_\phi^2 \\ & & \frac{\lambda_0}{2}\frac{v_\chi v_\phi^2}{v_{\Delta_1}} & 0 \\ & & & \frac{\sqrt{2}\lambda_0'}{4}\frac{v_\phi^2 v_\chi}{v_{\Delta_0}} \end{bmatrix}. \tag{A7}$$

[1] G. Aad *et al.* (ATLAS Collaboration), Phys. Lett. B **716**, 1 (2012); S. Chatrchyan *et al.* (CMS Collaboration), Phys. Lett. B **716**, 30 (2012).

[2] A. Zee, Phys. Lett. **93B**, 389 (1980); **95B**, 461 (1980).

[3] A. Zee, Phys. Lett. **161B**, 141 (1985); A. Zee, Nucl. Phys. **B264**, 99 (1986); K. S. Babu, Phys. Lett. B **203**, 132 (1988).

[4] L. M. Krauss, S. Nasri, and M. Trodden, Phys. Rev. D **67**, 085002 (2003).

[5] K. Cheung and O. Seto, Phys. Rev. D **69**, 113009 (2004); A. Ahriche, C.-S. Chen, K. L. McDonald, and S. Nasri, arXiv:1404.2696.

[6] A. Ahriche, S. Nasri, and R. Soualah, Phys. Rev. D **89**, 095010 (2014).

[7] E. Ma, Phys. Rev. D **73**, 077301 (2006).

[8] D. Schmidt, T. Schwetz, and T. Toma, Phys. Rev. D **85**, 073009 (2012).

[9] R. Bouchand and A. Merle, J. High Energy Phys. 07 (2012) 084.

[10] S. Kanemura, O. Seto, and T. Shimomura, Phys. Rev. D **84**, 016004 (2011); M. Aoki, J. Kubo, T. Okawa, and H. Takano, Phys. Lett. B **707**, 107 (2012); Y. Farzan and E. Ma, Phys. Rev. D **86**, 033007 (2012); F. Bonnet, M. Hirsch, T. Ota, and W. Winter, J. High Energy Phys. 07 (2012) 153; K. Kumericki, I. Picek, and B. Radovcic, J. High Energy Phys. 07 (2012) 039; K. Kumericki, I. Picek, and B. Radovcic, Phys. Rev. D **86**, 013006 (2012); E. Ma, Phys. Lett. B **717**, 235 (2012); G. Gil, P. Chankowski, and M. Krawczyk, Phys. Lett. B **717**, 396 (2012); H. Okada and T. Toma, Phys. Rev. D **86**, 033011 (2012); D. Hehn and A. Ibarra, Phys. Lett. B **718**, 988 (2013); P. S. B. Dev and A. Pilaftsis, Phys. Rev. D **86**, 113001 (2012); Y. Kajiyama, H. Okada, and T. Toma, Eur. Phys. J. C **73**, 2381 (2013).

[11] M. Aoki, S. Kanemura, and O. Seto, Phys. Rev. Lett. **102**, 051805 (2009).

[12] M. Aoki, S. Kanemura, and O. Seto, Phys. Rev. D **80**, 033007 (2009).

[13] M. Aoki, S. Kanemura, and K. Yagyu, Phys. Rev. D **83**, 075016 (2011).

[14] A. E. Nelson, D. B. Kaplan, and A. G. Cohen, Nucl. Phys. **B373**, 453 (1992); N. Turok and J. Zadrozny, Nucl. Phys. **B358**, 471 (1991); **B369**, 729 (1992); K. Funakubo, A. Kakuto, and K. Takenaga, Prog. Theor. Phys. **91**, 341 (1994); A. T. Davies, C. D. Froggatt, G. Jenkins, and R. G. Moorhouse, Phys. Lett. B **336**, 464 (1994); J. M. Cline, K. Kainulainen, and A. P. Vischer, Phys. Rev. D **54**, 2451 (1996); S. Kanemura, Y. Okada, and E. Senaha, Phys. Lett. B **606**, 361 (2005); L. Fromme, S. J. Huber, and M. Seniuch, J. High Energy Phys. 11 (2006) 038.

[15] S. Kanemura, T. Nabeshima, and H. Sugiyama, Phys. Lett. B **703**, 66 (2011); Phys. Rev. D **85**, 033004 (2012); S. Kanemura, T. Matsui, and H. Sugiyama, Phys. Lett. B **727**, 151 (2013); Phys. Rev. D **90**, 013001 (2014).

[16] P.-H. Gu and U. Sarkar, Phys. Rev. D **77**, 105031 (2008); **78**, 073012 (2008); M. Lindner, D. Schmidt, and T. Schwetz, Phys. Lett. B **705**, 324 (2011); M. Aoki, S. Kanemura, T. Shindou, and K. Yagyu, J. High Energy Phys. 07 (2010) 084; 11 (2010) 49E; M. Gustafsson, J. M. No, and M. A. Rivera, Phys. Rev. Lett. **110**, 211802 (2013); S. Kanemura and H. Sugiyama, Phys. Rev. D **86**, 073006 (2012); M. Aoki, J. Kubo, and H. Takano, Phys. Rev. D **87**, 116001 (2013); Y. Kajiyama, H. Okada, and K. Yagyu, Nucl. Phys. **B874**, 198 (2013); Y. Kajiyama, H. Okada, and T. Toma, Phys. Rev. D **88**, 015029 (2013); B. Dasgupta, E. Ma, and K. Tsumura, Phys. Rev. D **89**, 041702 (2014); A. E. Carcamo Hernandez, R. Martinez, and F. Ochoa, arXiv:1309.6567; S. Baek, H. Okada, and T. Toma, J. Cosmol. Astropart. Phys. 06 (2014) 027; E. Ma, Phys. Lett. B **732**, 167 (2014); S. Baek, H. Okada, and T. Toma, Phys. Lett. B **732**, 85 (2014); A. Ahriche, K. L. McDonald, and S. Nasri, arXiv:1404.5917; C.-S. Chen, K. L. McDonald, and S. Nasri, arXiv:1404.6033.

[17] Y. H. Ahn and H. Okada, Phys. Rev. D **85**, 073010 (2012); E. Ma, A. Natale, and A. Rashed, Int. J. Mod. Phys. A **27**, 1250134 (2012); Y. Kajiyama, H. Okada, and K. Yagyu, J. High Energy Phys. 10 (2013) 196; A. E. Carcamo Hernandez, I. de Medeiros Varzielas, S. G. Kovalenko, H. Päs, and I. Schmidt, Phys. Rev. D **88**, 076014 (2013); E. Ma and A. Natale, Phys. Lett. B **734**, 403 (2014).

[18] E. Ma, D. Ng, J. T. Pantaleone, and G.-G. Wong, Phys. Rev. D **40**, 1586 (1989); E. Ma, D. Ng, and G.-G. Wong, Z. Phys. C **47**, 431 (1990).

[19] F. R. Joaquim and J. T. Penedo, arXiv:1403.4925.

[20] A. Ibarra and A. Solaguren-Beascoa, arXiv:1403.2382.

[21] H. Okada and K. Yagyu, Phys. Rev. D **89**, 053008 (2014)

[22] M. Kakizaki, S. Kanemura, H. Taniguchi, and T. Yamashita, Phys. Rev. D **89**, 075013 (2014).

[23] M. S. Carena, A. Daleo, B. A. Dobrescu, and T. M. P. Tait, Phys. Rev. D **70**, 093009 (2004).

[24] A. V. Gulov and V. V. Skalozub, Phys. Rev. D **76**, 075008 (2007).

[25] D. V. Forero, M. Tortola, and J. W. F. Valle, Phys. Rev. D **86**, 073012 (2012).

[26] P. A. R. Ade *et al.* (Planck Collaboration), arXiv:1303.5076 [Astron. Astrophys. (to be published)].

[27] E. Aprile *et al.* (XENON100 Collaboration), Phys. Rev. Lett. **109**, 181301 (2012).

[28] D. S. Akerib *et al.* (LUX Collaboration), Phys. Rev. Lett. **112**, 091303 (2014).

[29] T. Hambye, F.-S. Ling, L. Lopez Honorez, and J. Rocher, J. High Energy Phys. 07 (2009) 090; 05 (2010) 066E.

[30] G. W. Bennett *et al.* (Muon g-2 Collaboration), Phys. Rev. D **73**, 072003 (2006).

[31] F. Jegerlehner and A. Nyffeler, Phys. Rep. **477**, 1 (2009).

[32] M. Benayoun, P. David, L. Delbuono, and F. Jegerlehner, Eur. Phys. J. C **72**, 1848 (2012).

[33] A. Pukhov, arXiv:hep-ph/0412191.

[34] T. P. Cheng and L. F. Li, Phys. Rev. D **22**, 2860 (1980); J. Schechter and J. W. F. Valle, Phys. Rev. D **22**, 2227 (1980); G. Lazarides, Q. Shafi, and C. Wetterich, Nucl. Phys. **B181**, 287 (1981); R. N. Mohapatra and G. Senjanovic, Phys. Rev. D **23**, 165 (1981); M. Magg and C. Wetterich, Phys. Lett. **94B**, 61 (1980).

[35] T. Han, B. Mukhopadhyaya, Z. Si, and K. Wang, Phys. Rev. D **76**, 075013 (2007); P. Fileviez Perez, T. Han, G.-Y. Huang, T. Li, and K. Wang, Phys. Rev. D **78**, 015018 (2008); C.-W. Chiang, T. Nomura, and K. Tsumura, Phys. Rev. D **85**, 095023 (2012); Z. Kang, J. Li, T. Li, Y. Liu, and G.-Z. Ning, arXiv:1404.5207.

[36] S. Kanemura, K. Yagyu, and H. Yokoya, Phys. Lett. B **726**, 316 (2013).